

Motion and collision of particles near DST Black holes

P. A. González* and Marco Olivares†

*Facultad de Ingeniería y Ciencias, Universidad Diego Portales,
Avenida Ejército Libertador 441, Casilla 298-V, Santiago, Chile.*

Ali Övgün‡

*Instituto de Física, Pontificia Universidad Católica de Valparaíso, Casilla 4950, Valparaíso, Chile. and
Physics Department, Arts and Sciences Faculty, Eastern Mediterranean University,
Famagusta, North Cyprus via Mersin 10, Turkey.*

Joel Saavedra§

Instituto de Física, Pontificia Universidad Católica de Valparaíso, Casilla 4950, Valparaíso, Chile.

Yerko Vásquez¶

*Departamento de Física y Astronomía, Facultad de Ciencias, Universidad de La Serena,
Avenida Cisternas 1200, La Serena, Chile.*

(Dated: March 22, 2019)

We consider Deser-Sarioglu-Tekin (DST) black holes as background and we study such the motion of massive particles as the collision of two spinning particles in the vicinity of its horizon. New kinds of orbits are allowed for small deviations of General Relativity, but the behavior of the collision is similar to the one observed for General Relativity. Some observables like bending of light and the perihelion precession are analyzed.

PACS numbers: 04.40.-b, 95.30.Sf, 98.62.Sb

Keywords: Geodesics, light deflection, particles collision, BSW process

*Electronic address: pablo.gonzalez@udp.cl

†Electronic address: marco.olivares@mail.udp.cl

‡Electronic address: ali.ovgun@pucv.cl; URL: <http://www.aovgun.com>

§Electronic address: joel.saavedra@ucv.cl

¶Electronic address: yvasquez@userena.cl

Contents

I. Introduction	3
II. DST black holes	4
III. Geodesics in the equatorial plane	5
A. Null geodesics	6
1. Radial motion	6
2. Angular motion	8
3. Bending of light	10
B. Time like geodesics	11
1. Radial geodesics	11
2. Angular geodesics	12
3. Perihelion precession	13
IV. Collisions of spinning particles near DST black holes	15
V. Conclusions	19
Acknowledgments	19
References	20

I. INTRODUCTION

The Deser-Sarioglu-Tekin (DST) action is characterized by the action of General Relativity (GR) with additional terms, i.e. non-polynomial terms of the Weyl tensor, that preserve the (first) derivative order of the GR equations in Schwarzschild gauge and provide non-Ricci flat extensions of GR. DST black holes are obtained using the Weyl technique for pure GR [2] which led to rather strange metrics [1], however GR can be recovered. Their thermodynamics was studied in [3].

The motion of particles in a spherically symmetric spacetime background has been of great interest. It is known that all solar system observations, such as light deflection, the perihelion shift of planets, the gravitational time-delay among other are well described within Einstein's General Relativity. Also, observational data allow us to fix the parameters of alternative four-dimensional theories, see for instance [4, 5]. In these regards, we address if new orbits appear as well as if the DST theory allows us to set the observables better than GR, for small deviation of GR. The study of the motion of spinning tops (STOPs) in the framework of GR began with the works of Mathisson [6] and Papapetrou [7], which was again taken by Tulczyjew [8], Taub [9], and Dixon [10]. The analysis of spinning particles moving around Schwarzschild black holes was first carried out by Corinaldesi and Papapetrou [11] solving the Mathisson-Papapetrou (MP) equations, and later by Hojman [12] solving the resulting equations derived from the Lagrangian formalism. An analytic treatment of the trajectories in general Schwarzschild-like spacetimes was carried out in [13], resulting that a spinning test particle does not follow geodesics, due to its interaction with tidal forces.

On the other hand, it is known that the black holes can act as natural particle accelerators if in a collisional process of two particles near the degenerate horizon of an extreme Kerr black hole, one of the particles has a critical angular momentum by creating a large center of mass (CM) energy [15]. Nowadays, this process is known as the Bañados, Silk and West (BSW) mechanism, which was found for the first time by Piran, Shaham and Katz in 1975 [16–18]. The BSW mechanism can be extended to non-extremal black holes [19, 23] and to non-rotating charged black holes [21]. On top of that, it has been argued to be a universal property of rotating black holes [20]. The BSW mechanism has been studied for different black hole geometries [25–28]. Also, the formation of black holes through the BSW mechanism was investigated in [29]. It is worth to mention that for the collision of STOPs in the equatorial plane of a Schwarzschild black hole it was found that retrograde trajectories can experience significant accelerations, which generate divergent center-of-mass energies if the STOP collides with another particle moving in the same plane. However, in order to reach such divergence the trajectory of the STOP has to pass from timelike to spacelike [30]. In this regards, we address if the DST black hole can acts as a particle accelerators.

The manuscript is organized as follows: In Sec. II we give a brief review of the DST black hole. Then, we study and discuss about the geodesics in the equatorial plane, and we analyze two observables, in particular the bending of the light and the perihelion precession. Also, we find the values of the coupling parameter in order to set the observations in both test, in Sec. III. Then, in Sec. IV we study the collision of spinning particles and we investigate the possibility that the DST black hole acts as a particle accelerator. Finally, our conclusions are in Sec. V.

II. DST BLACK HOLES

The action of Deser-Sarioglu-Tekin [1] corresponds to the Einstein action with the addition of non-polynomial terms, which in units of $\kappa = 1$ is given by

$$I = \frac{1}{2} \int d^4x \sqrt{-g} \left(R + \beta_n |trC^n|^{1/n} \right), \quad (1)$$

where

$$trC^n \equiv C_{ab}{}^{cd} C_{cd}{}^{ef} \dots C_{..}{}^{pq} C_{pq}{}^{ab} \dots, \quad (2)$$

being n the number of copies of the Weyl tensor C and β_n corresponds to the coupling constant. So, for $n=2$ and by defining $\sigma = \beta_2/\sqrt{3}$, the above action can be written as

$$I = \int_0^\infty dr [(1 - \sigma)(arb' + b) + 3\sigma ab], \quad (3)$$

up to boundary terms. Here, primes denote radial derivatives. Thus, for $D = 4$, the following metric is solution of the field equations

$$ds^2 = -a(r) b^2(r) dt^2 + \frac{dr^2}{a(r)} + r^2 d\Omega_2. \quad (4)$$

where

$$a(r) = \frac{1 - \sigma}{1 - 4\sigma} + a_1 r^{(4\sigma-1)/(1-\sigma)}, \quad b(r) = b_1 r^{3\sigma/(\sigma-1)}, \quad (5)$$

a_1 and b_1 are integration constants of which b_1 is removable by time rescaling. Note that for $\sigma = 1$, there is no solution at all, for $\sigma = 0$ GR is recovered, and for $\sigma = 1/4$, $a(r) = \ln(r/r_0)$ and $b(r) = 1/r$. All nonvanishing components of the mixed Weyl tensor are proportional to the single function X

$$X(r, t) \equiv \frac{1}{r^2} \left(2(a - 1) - 2ra' + r^2 a'' \right) + \frac{1}{rb} \left(3ra'b' - 2a(b' - rb'') \right) + \frac{1}{b} \partial_t \left(\frac{1}{a^2 b} \partial_t a \right), \quad (6)$$

where primes denote radial derivatives. Also, any scalar of order n in the Weyl tensor C is proportional to X^n . Therefore

$$trC^n = \left(-\frac{1}{3} \right)^n [2 + (-2)^{2-n}] X^n. \quad (7)$$

Note that the range $1/4 < \sigma < 1$ is excluded to retain the signature. However, for $a_1 < 0$, is possible to recover the Schwarzschild metric. In the following we analyze de branch $a_1 < 0$, and we consider the functions $a(r)$ and $b(r)$ as

$$a(r) = \frac{1 - \sigma}{1 - 4\sigma} - \left(\frac{r_S}{r} \right)^{\frac{1-4\sigma}{1-\sigma}}, \quad (8)$$

$$b(r) = \left(\frac{r}{r_S} \right)^{\frac{3\sigma}{\sigma-1}}, \quad (9)$$

that are dimensionless, with r_S being the Schwarzschild horizon coordinate. The black hole horizon is given by

$$r_+(\sigma, r_S) = r_S \left(\frac{1 - 4\sigma}{1 - \sigma} \right)^{\frac{1-\sigma}{1-4\sigma}}, \quad (10)$$

that depends on the parameter σ and the Schwarzschild's horizon. The event horizon, as a function of σ , has a maximum value $r_+^{(max)} \approx 1.44r_S$ when

$$\sigma_1 = -\frac{e-1}{4-e} \approx -1.34. \quad (11)$$

Also, when $\sigma \rightarrow \pm\infty$, $r_+ \rightarrow \sqrt{2}r_S$, see Fig. 1.

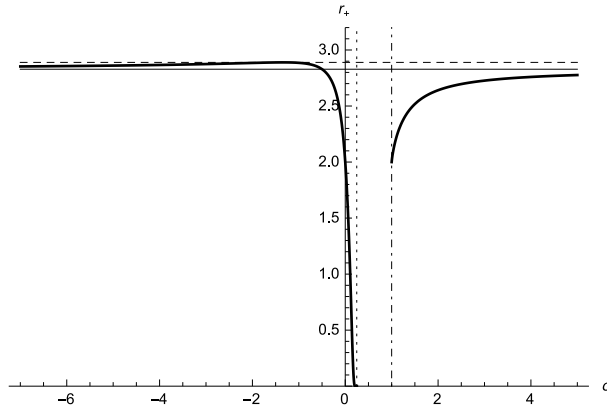


FIG. 1: The behavior of the DST horizon as a function of σ with $r_S = 2$.

III. GEODESICS IN THE EQUATORIAL PLANE

The Lagrangian associated to the metric (4) is

$$2\mathcal{L} = -ab^2\dot{t}^2 + \frac{\dot{r}^2}{a} + r^2\dot{\theta}^2 + r^2\sin^2\theta\dot{\phi}^2, \quad (12)$$

where $\dot{q} = dq/d\lambda$, and λ is an affine parameter along the geodesic that we choose as the proper time τ for particles. Since the Lagrangian (12) is independent of the coordinates (t, ϕ) , then their conjugate momenta (Π_t, Π_ϕ) are conserved. The equations of motion can be obtained from

$$\dot{\Pi}_q - \frac{\partial \mathcal{L}}{\partial q} = 0, \quad (13)$$

which yield

$$\dot{\Pi}_t = 0, \quad \dot{\Pi}_r = -\frac{\dot{t}^2 d(ab^2)}{2 dr} + \frac{\dot{r}^2 d(a^{-1})}{2 dr} + r\dot{\theta}^2 + r\sin^2\theta\dot{\phi}^2, \quad (14)$$

$$\dot{\Pi}_\theta = r^2\sin\theta\cos\theta\dot{\phi}^2, \quad \text{and} \quad \dot{\Pi}_\phi = 0. \quad (15)$$

where $\Pi_q = \partial\mathcal{L}/\partial\dot{q}$ are the conjugate momenta to the coordinate q , in particular

$$\Pi_t = -a b^2 \dot{t}, \quad \Pi_r = \frac{\dot{r}}{a}, \quad (16)$$

$$\Pi_\theta = \dot{r}^2 \dot{\theta}, \quad \text{and} \quad \Pi_\phi = r^2 \sin^2 \theta \dot{\phi}. \quad (17)$$

So, by considering the motion of neutral particles on the equatorial plane: $\theta = \pi/2$ and $\dot{\theta} = 0$, we obtain

$$\Pi_t = -a b^2 \dot{t} \equiv -E, \quad \Pi_r = \frac{\dot{r}}{a}, \quad \Pi_\phi = r^2 \dot{\phi} \equiv L, \quad (18)$$

where E and L_ϕ are integration constants dimensionless. Now, by using equations (8) and (11), the Lagrangian can be rewritten in the following form:

$$2\mathcal{L} \equiv -m = -\frac{E^2}{a b^2} + \frac{\dot{r}^2}{a} + \frac{L^2}{r^2}. \quad (19)$$

So, by normalization, we shall consider that $m = 1$ for massive particles and $m = 0$ for photons. We solve the above equation for \dot{r}^2 in order to obtain the radial equation, which allows us to characterize the possible movements of test particles without an explicit solution of the equation of motion in the invariant plane, and we obtain

$$\left(\frac{dr}{d\lambda}\right)^2 = \frac{1}{b^2} [E^2 - V(r)], \quad (20)$$

$$\left(\frac{dr}{dt}\right)^2 = \frac{a^2 b^2}{E^2} [E^2 - V(r)], \quad (21)$$

$$\left(\frac{dr}{d\phi}\right)^2 = \frac{r^4}{L^2 b^2} [E^2 - V(r)], \quad (22)$$

where $V(r)$ is the effective potential given by

$$V(r) = a b^2 \left(m + \frac{L^2}{r^2}\right). \quad (23)$$

A. Null geodesics

1. Radial motion

The radial motion corresponds to a trajectory with null angular momentum (or zero impact parameter). In this case, the photons are destined to escape at the infinity or fall into the black hole due to the effective potential is $V(r) = 0$. Also, Eqs. (21) and (22) reduce to

$$\pm \frac{dr}{d\lambda} = \frac{E}{b}, \quad (24)$$

and

$$\pm \frac{dr}{dt} = a b, \quad (25)$$

respectively. The sign $+$ ($-$) corresponds to photons that escape (falling) from the event horizon. Now, choosing the initial conditions for the photons as $r = \rho_0$ when $t = \lambda = 0$, the Eq. (24) yields

$$\lambda(r) = \pm \frac{r_S}{E} \left(\frac{1 - \sigma}{1 - 4\sigma} \right) \left[\left(\frac{r}{r_S} \right)^{\frac{1-4\sigma}{1-\sigma}} - \left(\frac{\rho_0}{r_S} \right)^{\frac{1-4\sigma}{1-\sigma}} \right]. \quad (26)$$

Thus, the photons arrive to the event horizon in a finite λ parameter, which can be observed in Fig. 2. Notice that for photons plunge to the horizon, with the same energy. The photon in the neighborhood of a DST black hole with positive σ ($0 < \sigma < 1/4$) reaches a point (outside the horizon) in a less affine parameter that a photon in the neighborhood of a DST black hole with a negative σ .

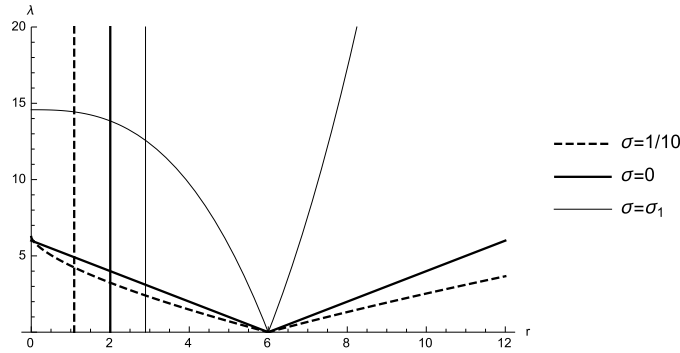


FIG. 2: The behavior of the affine parameter λ as a function of r , for different values of σ , with $E = 1$, $\rho_0 = 6$, $r_S = 2$. Vertical lines correspond to the event horizon for different σ values.

On the other hand, performing the change of variables $x = (r/r_+)^{\nu+1}$, and integrating Eq. (25) leads to

$$t(r) = \pm r_S \left(\frac{r_+}{r_S} \right)^{1-\nu} (B[x; z + 1, 0] - B[x_0; z + 1, 0]), \quad (27)$$

where $B[x; \bar{\alpha}, \bar{\beta}]$ corresponds to the Beta function, $z = (1 - \nu)/(1 + \nu)$ and $(1 - \sigma)/(1 - 4\sigma) = 1/(1 + \nu)$. Notice that the solution for the coordinate time does not depend on the energy of the photon. In Fig. 3, we can observe that the photons in the coordinate time not cross the horizon of the DST black holes.

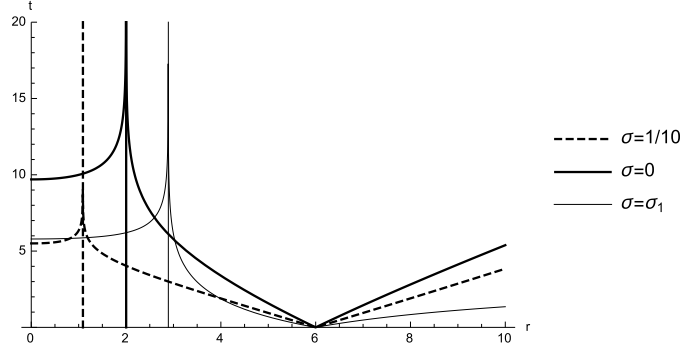


FIG. 3: The behavior of the coordinate time t as a function of r , for different values of σ , with $\rho_0 = 6$, and $r_S = 2$. Vertical lines correspond to the event horizon for different σ values.

2. Angular motion

The effective potential for photons and their trajectories, are plotted in Fig. 4. The effective potential presents a maximum value, that correspond to a unstable circular orbit with a radius given by

$$r_U = r_S \left(\frac{3(1-4\sigma)}{2(1-\sigma)(1+2\sigma)} \right)^{\frac{1-\sigma}{1-4\sigma}}. \quad (28)$$

The classical result for the Schwarzschild's spacetime ($r_U = 3M$) is obtained when $\sigma = 0$, and $r_S = 2M$. It is worth mentioning that there is a maximum in the potential only for $-1/2 < \sigma < 1/4$. On the other hand, the potential shows a different behavior for $\sigma \leq -1/2$.

Now, based on the impact parameter values $\beta \equiv L/E$, we give a brief qualitative description of the allowed angular motions for photons plotted in Fig. 4. First, we can observe a *capture zone*, if $0 < \beta < \beta_c$, where $\beta_c = L/E_c$ with $E_c = V(r_U)$, where the photons fall on the horizon, depending on initial conditions, and its cross section, $\bar{\sigma}$, in these geometry is [39]

$$\bar{\sigma} = \pi \beta_c^2. \quad (29)$$

Also, we can observe a *critical trajectories*, if $\beta = \beta_c$, where the photons can stay in one of the unstable circular orbit of radius r_U . Therefore, the photons that arrive from an initial distance r_i ($r_+ < r_i < r_U$) can asymptotically fall to a circle of radius r_U . The proper period in such orbit is

$$T_\tau = \frac{2\pi r_U^2}{L}. \quad (30)$$

It results to be the same as the one in the Schwarzschild case [40], when $\sigma = 0$. Also, the coordinate period is given by

$$T_t = 2\pi \beta_c. \quad (31)$$

Finally, there is a *deflection zone*, if $\beta_c < \beta_d < \infty$, where the photons come from infinity to a distance $r = r_d$ (which is solution of the equation $V(r_d) = E$), then return to the infinity.

As we mentioned, the potential shows a different behavior for $\sigma \leq -1/2$. While that for $\sigma = -1/2$, the potential tends to $L^2/2$, for $\sigma < -1/2$ the potential shows that all trajectories allowed have a return point and then plunge into the black hole, see Fig. 5.

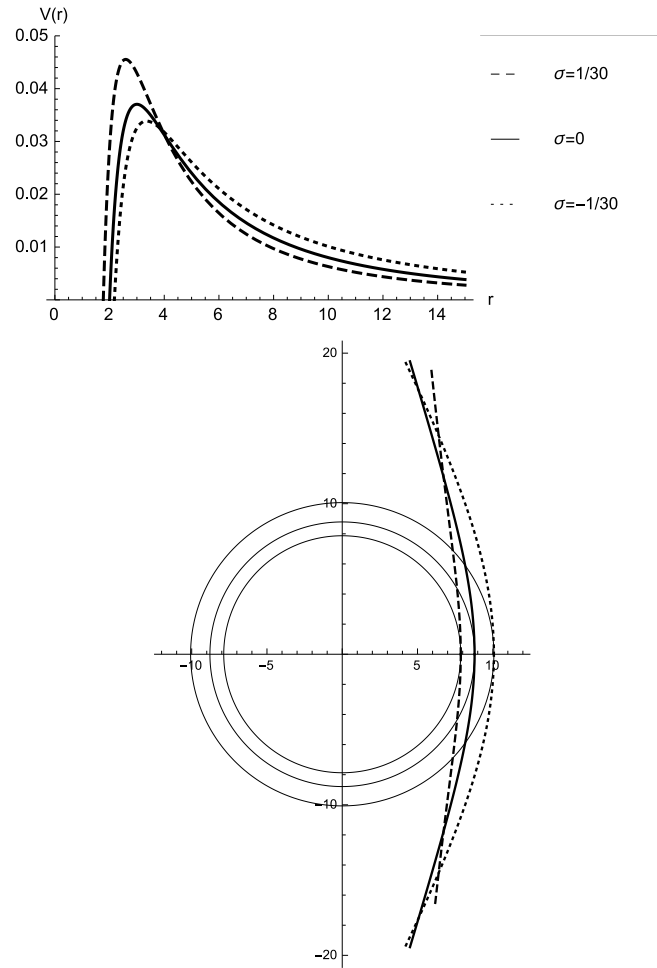


FIG. 4: The top panel shows the behavior of the effective potential for photons $V(r)$ as a function of r , for different values of σ , with $r_S = 2$ and $L = 1$. The bottom panel shows the trajectories for photons with $E^2 = 0.01$, and different values of σ .

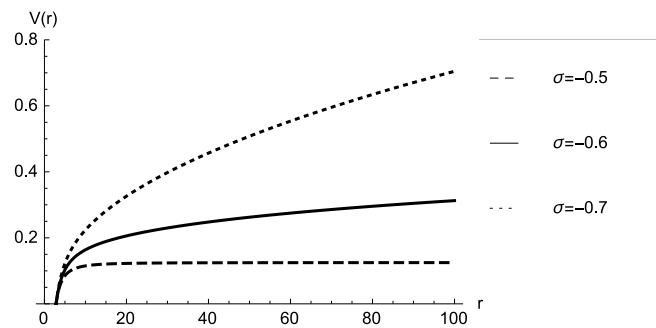


FIG. 5: The behavior of the effective potential for photons $V(r)$ as a function of r , for $\sigma \leq -1/2$, with $r_S = 2$ and $L = 1$.

3. Bending of light

In this section we will follow the procedure establish in Ref. [35]. So, Eq. (22) for photons is

$$\left(\frac{dr}{d\phi}\right)^2 = \frac{r_S^{2\nu}}{\beta^2} r^{4-2\nu} - \mu r^2 + r_S^{1/\mu} r^{1-\nu}, \quad (32)$$

where β is the impact parameter, $\nu = 3\sigma/(\sigma - 1)$ and $\mu = (1 - \sigma)/(1 - 4\sigma)$. By using the change of variables $r = 1/u$, the above equation can be written as

$$\left(\frac{du}{d\phi}\right)^2 = \frac{r_S^{2\nu}}{\beta^2} u^{2\nu} - \mu u^2 + r_S^{1/\mu} u^{3+\nu}. \quad (33)$$

Notice that for $\sigma = 0$, the above equation is reduced to the classical equation of Schwarzschild for the motion of photons for $r_S = 2M$

$$\left(\frac{du}{d\phi}\right)^2 = \frac{1}{\beta^2} - u^2 + 2Mu^3. \quad (34)$$

So, the derivate of Eq. (33) with respect ϕ yields

$$u'' + \mu u = \frac{r_S^{1/\mu}}{2} (3 + \nu) u^{2+\nu} + \frac{\nu r_S^{2\nu}}{\beta^2} u^{2\nu-1}, \quad (35)$$

where $'$ denotes the derivative with respect to ϕ . Now, neglecting the last term, we obtain

$$u = \frac{1}{\beta} \sin(\sqrt{\mu}\phi) + \frac{\epsilon}{\beta^{2+\nu} 2^{1+\nu/2} \mu} \left(1 + \frac{2+\nu}{6} \cos(2\sqrt{\mu}\phi)\right), \quad (36)$$

where $\epsilon = r_S^{1/\mu} (3 + \nu)/2$. For large r (small u), ϕ is small, and we may take $\sin(\sqrt{\mu}\phi) \approx \sqrt{\mu}\phi$ and $\cos(2\sqrt{\mu}\phi) \approx 1$. In the limit $u \rightarrow 0$, ϕ approaches ϕ_∞ , with

$$\phi_\infty = -\frac{(3 + \nu)(8 + \nu) r_S^{1/\mu}}{6\mu^{3/2} \beta^{1+\nu} 2^{2+\nu/2}}. \quad (37)$$

Therefore, for the DST black holes the deflection of light $\hat{\alpha}$ is equal to $2|\phi_\infty|$ and yields

$$\hat{\alpha} = \frac{(3 + \nu)(8 + \nu)}{3\mu^{3/2} 2^{2+\nu/2}} \left(\frac{r_s}{\beta}\right)^{1+\nu}. \quad (38)$$

Notice that for $\sigma = 0$, and $r_S = 2M$ we recovered the classical result of GR, that is, $\hat{\alpha} = 4M/\beta$. The first observational value of deflection light was measured by Eddington and Dyson in the solar eclipse of March 29, 1919. For Sobral expedition this value is $\hat{\alpha}_{Obs.} = 1.98 \pm 0.16''$ and $\hat{\alpha}_{Obs.} = 1.61 \pm 0.40''$ for the Principe expedition [35]. Nowadays, the parameterized post-Newtonian (PPN) formalism introduce the phenomenological parameter γ , that characterizes the contribution of space curvature to gravitational deflection, in this formalism the deflection angle $\hat{\alpha} = 0.5(1 + \gamma)1.7426$, and currently $\gamma = 0.9998 \pm 0.0004$ [41]. So, $\hat{\alpha} = 1.74277''$ for $\gamma = 0.9998 + 0.0004$ and $\hat{\alpha} = 1.74208''$ for $\gamma = 0.9998 - 0.0004$.

It is worth to mention that there is a discrepancy between the theoretical value predicted by GR and the observational value. So, by attributing this discrepancy to small deviations of Schwarzschild's spacetime, we can attribute such discrepancy to σ . Therefore, $-8.97241 \times 10^{-6} < \sigma < 3.41708 \times 10^{-6}$, in order to mach with the observational results.

B. Time like geodesics

In this section, we will study the motion of massive particles and the perihelion precession. In the following, we fix $m = 1$.

1. Radial geodesics

The effective potential for particles ($L = 0$) is plotted in Fig. 6. Notice that, for $\sigma = 0$, there are two kind of trajectories. One of them is the bounded trajectory ($E < 1$), which has a return point and plunge into the horizon. The other one, is the unbounded trajectory ($E \geq 1$), which can escape at the infinity or plunge into the black hole. For $\sigma < 0$, we observe that the allowed trajectories are bounded. Interestingly, for $0 < \sigma < 1/4$, the potential has a maximum value $V(r_u) \equiv E_u^2$, at the unstable equilibrium point (r_u), that it is not present in GR ($\sigma = 0$), and it can be obtained from the derivative of Eq. (23) with respect to r . This unstable equilibrium point, is given by

$$r_u = r_S \left(\frac{(1 - 4\sigma)(1 + 2\sigma)}{6\sigma(1 - \sigma)} \right)^{\frac{1-\sigma}{1-4\sigma}}. \quad (39)$$

Also, for this range of values of σ , there are three kind of trajectories. The first, are the critical trajectories, of first and second kind, which are allows for particles with $E = E_u$. The trajectories of first kind are characterized for particles that incoming from the infinity to the unstable equilibrium point, asymptotically. The trajectories of second kind are characterized for particles that incoming from a distance, $r < r_u$, to the unstable equilibrium point, asymptotically. For, particles with $E > E_u$, the trajectories are unbounded, and for $E < E_u$, we observe that is allow a frontal scattering, that is characterized for particles that incoming from infinity to a radial distance of closest approach, and come back to the infinity. The frontal scattering for charged particles was studied in Ref. [36].

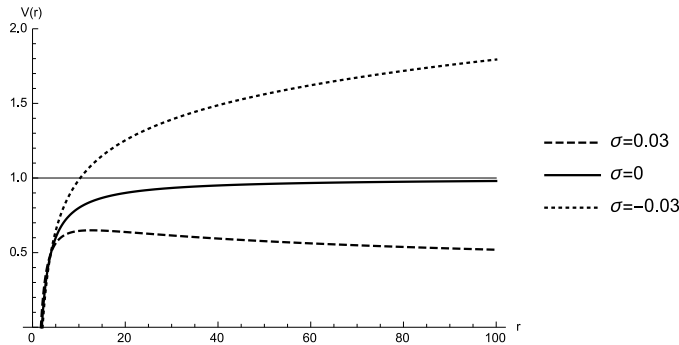


FIG. 6: The behavior of the effective potential for particles $V(r)$ as a function of r , for different values of σ , $r_S = 2$ and $L = 0$. For $\sigma = 0$ the potential $V(\infty) = 1$, for $\sigma < 0$ the potential $V(\infty) = \infty$, and for $0 < \sigma < 1/4$ the potential $V(\infty) = 0$.

2. Angular geodesics

The effective potential for particles with positive angular momentum is plotted in Fig. 7. Note that, for the cases that have been analyzed the effective potential has a maximum and a minimum value, which corresponds to a unstable and stable circular orbit, respectively. Also, there are bound orbits like planetary orbits, as in GR [42], for instance see left panel of Fig. 8 for a positive σ . Moreover, for $\sigma < 0$, all the trajectories are bounded due to $V(\infty) = \infty$. It is worth mention that these kind of orbits have the same behavior that the time like orbits for Schwarzschild AdS black hole [37]. Interestingly, for $0 < \sigma < 1/4$, the spacetime allow two unstable circular orbits and one stable circular orbit. In the right panel of Fig. 7, we show the scattering of neutral particles with $E < 1$, that are not present in the Schwarzschild spacetime, which can be a repulsive scattering or an attractive scattering.

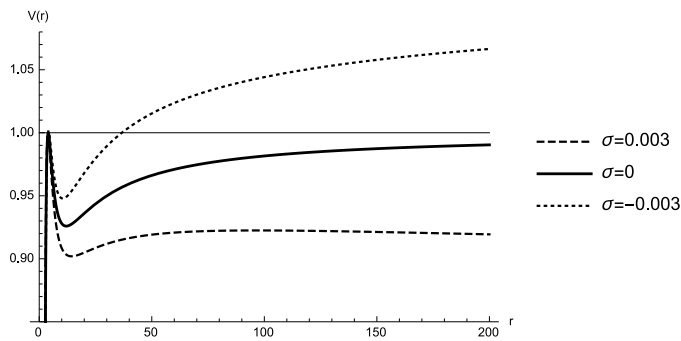


FIG. 7: The behavior of the effective potential for particles $V(r)$ as a function of r , for different values of σ , with $r_S = 2$ and $L = 4$. For $\sigma = 0$ the potential $V(\infty) = 1$, for $\sigma < 0$ the potential $V(\infty) = \infty$, and for $0 < \sigma < 1/4$ the potential $V(\infty) = 0$.

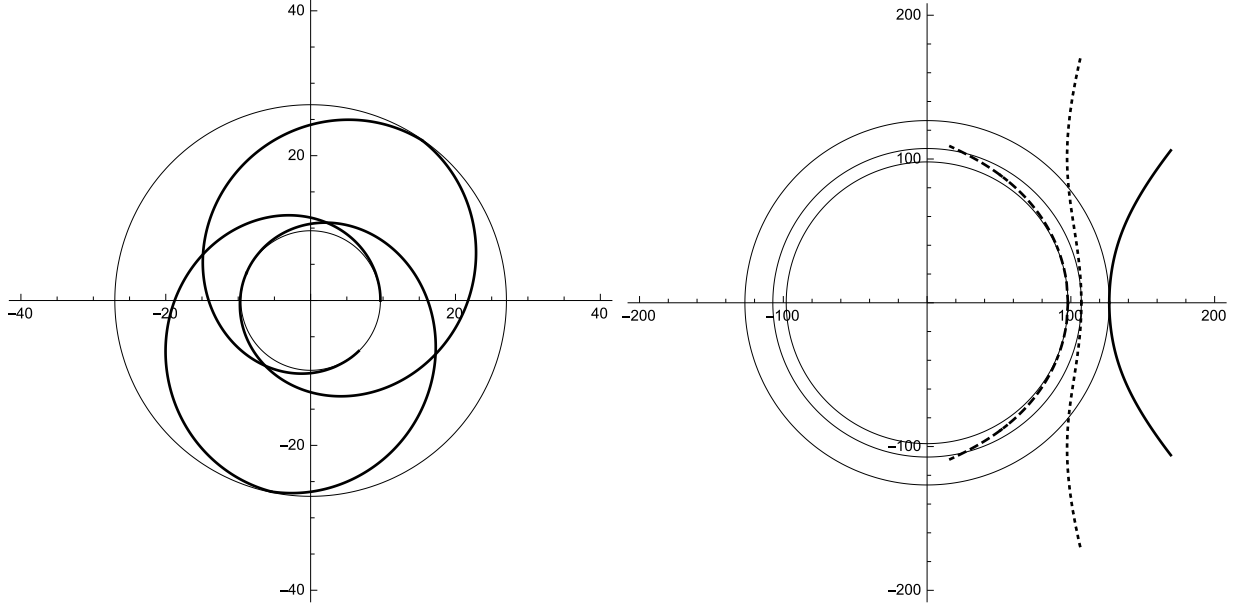


FIG. 8: Trajectories of particles with angular momentum $L = 4$ in the background of DST black hole with $r_S = 2$ and $\sigma = 0.003$. Left panel for bounded orbits like planetary orbit with energy $E^2 = 0.91$. Right panel for the scattering of neutral particles with different values of energy, the continuous line corresponds to $E^2 = 0.922$ (repulsive scattering), the dashed line corresponds to $E^2 = 0.92247$ (attractive scattering) and the dotted line corresponds to $E^2 = 0.9224$.

3. Perihelion precession

The previous analysis of effective potential for particles showed that there are planetary orbits, which allow us study the perihelion precession. So, we follow the treatment performed by Cornbleet [38], which allows us to derive the formula for the advance of the perihelia of planetary orbits. The starting point is to consider the line element in unperturbed Lorentz coordinates

$$ds^2 = -dt^2 + dr^2 + r^2(d\theta^2 + \sin^2\theta d\phi^2), \quad (40)$$

together with line element (4). So, considering only the radial and time coordinates in the binomial approximation, and $b(r) \approx 1$, when $\sigma \rightarrow 0$ in the Newtonian limit. So, the transformation gives

$$d\tilde{t} \approx \sqrt{\mu} \left(1 - \frac{1}{2\mu} \left(\frac{r_S}{r} \right)^{\frac{1}{\mu}} \right) dt, \quad (41)$$

$$d\tilde{r} \approx \frac{1}{\sqrt{\mu}} \left(1 + \frac{1}{2\mu} \left(\frac{r_S}{r} \right)^{\frac{1}{\mu}} \right) dr. \quad (42)$$

We will consider two elliptical orbits, one the classical Kepler orbit in (r, t) space and a DST black hole orbit in (\tilde{r}, \tilde{t}) space. Then, in the Lorentz space $dA = \int_0^{\mathcal{R}} r dr d\phi = \mathcal{R}^2 d\phi / 2$, and hence

$$\frac{dA}{dt} = \frac{1}{2} \mathcal{R}^2 \frac{d\phi}{dt}, \quad (43)$$

which corresponds to Kepler's second law. For the DST black hole case we have

$$d\tilde{A} = \int_0^{\mathcal{R}} r d\tilde{r} d\phi, \quad (44)$$

where $d\tilde{r}$ is given by Eq. (42). So, we can write (44) as

$$\begin{aligned} d\tilde{A} &= \frac{1}{\sqrt{\mu}} \int_0^{\mathcal{R}} r \left(1 + \frac{1}{2\mu} \left(\frac{r_S}{r} \right)^{1+\nu} \right) dr d\phi \\ &= \frac{1}{2\sqrt{\mu}} \left(\mathcal{R}^2 + \frac{r_S^{1+\nu} \mathcal{R}^{1-\nu}}{\mu(1-\nu)} \right) d\phi. \end{aligned} \quad (45)$$

Therefore, applying the binomial approximation we obtain

$$\begin{aligned} \frac{d\tilde{A}}{d\tilde{t}} &= \frac{1}{2\sqrt{\mu}} \left(\mathcal{R}^2 + \frac{r_S^{1+\nu} \mathcal{R}^{1-\nu}}{\mu(1-\nu)} \right) \frac{d\phi}{d\tilde{t}} \\ &\approx \frac{\mathcal{R}^2}{2\mu} \left(1 + \frac{(3-\nu)}{2\mu(1-\nu)} \left(\frac{r_S}{\mathcal{R}} \right)^{1+\nu} \right) \frac{d\phi}{dt}. \end{aligned} \quad (46)$$

So, using this increase to improve the elemental angle from $d\phi$ to $d\tilde{\phi}$. Then, for a single orbit

$$\int_0^{\Delta\tilde{\phi}} d\tilde{\phi} = \int_0^{\Delta\phi=2\pi} \frac{1}{\mu} \left(1 + \frac{(3-\nu)}{2\mu(1-\nu)} \left(\frac{r_S}{\mathcal{R}} \right)^{1+\nu} \right) d\phi. \quad (47)$$

Now, as the polar form of an ellipse is given by

$$\mathcal{R} = \frac{l}{1 + \epsilon \cos\phi}, \quad (48)$$

where ϵ is the eccentricity and l is the semi-latus rectum; and by plugging Eq. (48) into Eq. (47), we obtain

$$\Delta\tilde{\phi} = \frac{1}{\mu} \left(2\pi + \frac{(3-\nu)r_S^{1+\nu}}{2\mu(1-\nu)} \int_0^{2\pi} \left(\frac{1 + \epsilon \cos\phi}{l} \right)^{(1+\nu)} d\phi \right), \quad (49)$$

which at first order yields

$$\Delta\tilde{\phi} \approx \frac{1}{\mu} \left(2\pi + \frac{\pi(3-\nu)}{\mu(1-\nu)} \left(\frac{r_S}{l} \right)^{1+\nu} \right). \quad (50)$$

Notice that $\sigma = 0$, and $r_S = 2M$ we recover the classical result of GR. It is worth to mention that there is a discrepancy between the observational value of the precession of perihelion for Mercury, $\Delta\tilde{\phi}_{Obs.} = 5599.74$ (*arcsec/Julian - century*) and the total $\Delta\tilde{\phi} = \Delta\phi_{eq} + \Delta\phi_{pl} + \Delta\phi_{obl} = 5603.24$ (*arcsec/Julian - century*), where the term $\Delta\phi_{eq}$ is caused by the general precession in longitude, the term $\Delta\phi_{pl}$ is caused by the gravitational tugs of the other planets, and the term $\Delta\phi_{obl}$ is caused by the oblateness of the Sun [4]. Which, is possible attribute to a DST theory with $\sigma = 1.244 * 10^{-9}$.

IV. COLLISIONS OF SPINNING PARTICLES NEAR DST BLACK HOLES

The equations of motion derived from the Lagrangian theory for a spinning particle is given by [12, 14]

$$\frac{DP^\mu}{D\tau} = -\frac{1}{2}R_{\nu\alpha\beta}^\mu u^\nu S^{\alpha\beta}, \quad (51)$$

$$\frac{DS^{\mu\nu}}{D\tau} = S^{\mu\beta}\sigma_\beta^\nu - \sigma^{\mu\beta}S_\beta^\nu = P^\mu u^\nu - u^\mu P^\nu, \quad (52)$$

where $D/D\tau \equiv u^\mu \nabla_\mu$ is the covariant derivative along the velocity vector u^μ , τ is an affine parameter, P^μ is the canonical momentum, $R_{\nu\alpha\beta}^\mu$ is the Riemann tensor, $u^\mu = dX^\mu/d\tau$ is the tangent vector to the trajectory, $S^{\mu\nu}$ is the canonical spin tensor, and $\sigma^{\mu\nu}$ is the angular velocity. Spinning test particles in cosmological and static spherically symmetric spacetimes have been studied in [13]. Also, the collision of spinning particles near a Schwarzschild black hole was analyzed in [30]. In the following, we will consider the motion of spinning particles in the equatorial plane, that is, $\theta = \pi/2$ and $P^\theta = 0$. The modulus of the antisymmetric spin tensor and the mass of the particle are conserved quantities and are given respectively by

$$S^2 = \frac{1}{2}S_{\mu\nu}S^{\mu\nu}, \quad (53)$$

$$m^2 = -P_\mu P^\mu. \quad (54)$$

Other constants of motion are given by

$$Q_\xi = P^\mu \xi_\mu - \frac{1}{2}S^{\mu\nu} \nabla_\nu \xi_\mu, \quad (55)$$

where ξ^μ is a Killing vector of the space-time. The conserved quantity associated to the Killing vector ∂_t corresponds to the energy of the top and is found to be

$$E = a(r)b^2(r)P^t - \frac{1}{2}S^{tr} \left(a'(r)b^2(r) + 2a(r)b(r)b'(r) \right). \quad (56)$$

While, the conserved quantity associated to ∂_ϕ corresponds to the angular momentum of the top

$$J = r^2 P^\phi + r S^{r\phi}. \quad (57)$$

Also, the Tulczyjew constraint restrict the spin tensor to generate rotations only:

$$S^{\mu\nu} P_\nu = 0. \quad (58)$$

Thus, using the above equations, we find that the non-vanishing components of the momentum are given by

$$\frac{P^t}{m} = \frac{er^3 - \frac{jsr^2}{2b} (a'b^2 + 2abb')}{ab^2\Sigma}, \quad (59)$$

$$\frac{P^\phi}{m} = \frac{jr - \frac{esr}{b}}{\Sigma}, \quad (60)$$

and

$$\frac{P^r}{m} = \pm \sqrt{a^2 b^2 \left(\frac{P^t}{m} \right)^2 - ar^2 \left(\frac{P^\phi}{m} \right)^2 - a}, \quad (61)$$

where $e = E/m$ is the specific energy, $j = J/m$ is the total angular momentum per unit mass and $s = \pm S/m$ is the spin per unit mass. While, a positive value of the spin means that the spin is parallel to the total angular momentum, a negative value means that the spin is antiparallel to the total angular momentum. Also, Σ is given by

$$\begin{aligned}\Sigma &= r^3 - \frac{s^2 r^2}{2} \left(a' + 2a \frac{b'}{b} \right) \\ &= r^3 - \frac{s^2}{2} \left(r \Delta' - \left(1 - 2r \frac{b'}{b} \right) \Delta \right),\end{aligned}\quad (62)$$

where we have defined $\Delta = ra(r)$. Thus, by considering that the center of mass energy is given by

$$E_{CM}^2 = -g_{\mu\nu} (P_1^\mu + P_2^\mu) (P_1^\nu + P_2^\nu) = m_1^2 + m_2^2 - 2g_{\mu\nu} P_1^\mu P_2^\nu, \quad (63)$$

then the collisional energy for two spinning particles with the same mass $m = m_1 = m_2$ in the background of the DST black hole yields

$$\begin{aligned}E_{CM}^2 &= \frac{2m^2}{\Delta \Sigma_1 \Sigma_2} \left(\frac{r}{b^2} \left(e_1 r^3 - \frac{j_1 s_1}{2} r^2 (a'b + 2ab') \right) \left(e_2 r^3 - \frac{j_2 s_2}{2} r^2 (a'b + 2ab') \right) + \right. \\ &\quad \Delta \left(\Sigma_1 \Sigma_2 - r^4 (j_1 - e_1 s_1/b) (j_2 - e_2 s_2/b) \right) - \\ &\quad \frac{1}{b^2} \sqrt{r \left(e_1 r^3 - \frac{j_1 s_1}{2} r^2 (a'b + 2ab') \right)^2 - \Delta b^2 (\Sigma_1^2 + r^4 (j_1 - e_1 s_1/b)^2)} \times \\ &\quad \left. \sqrt{r \left(e_2 r^3 - \frac{j_2 s_2}{2} r^2 (a'b + 2ab') \right)^2 - \Delta b^2 (\Sigma_2^2 + r^4 (j_2 - e_2 s_2/b)^2)} \right). \quad (64)\end{aligned}$$

Possible divergences can arise when the denominator of the above equation is zero, i.e., at the horizon radius $\Delta = 0$ and at a spin-related radius $\Sigma_i = 0$. In the first case, it can be demonstrated that the CM energy is finite at the horizon. In fact, setting $s_i = 0$ for simplicity in the above expression with $i = 1, 2$, the E_{CM}^2 yields the finite value

$$\lim_{r \rightarrow r_H} \frac{E_{CM}^2}{m^2} = \frac{(e_2 j_1 - e_1 j_2)^2 + (e_1 + e_2)^2 r_H^2}{e_1 e_2 r_H^2}. \quad (65)$$

In the case $s_i \neq 0$ is more difficult to find an analytic expression like the above expression; However, it can be shown that E_{CM}^2 also is finite when $\Delta \rightarrow 0$. For instance, in Fig. (9) we can see that the CM energy does not diverge at the horizon for some particular values of the parameters. On the other hand, when $\Sigma_i \rightarrow 0$ the E_{CM}^2 diverges, indicating an infinite CM energy at the spin-related radius, this behavior is shown in the same Fig. (9) for some values of the parameters, which show that the divergence of the CM energy occurs outside the event horizon. However, it must be analyzed if the spinning particles can reach the divergence radius. In [30] was showed that for the Schwarzschild black hole some particles with retrograde orbits in principle can reach the divergence radius before reaching the horizon. Now, rewriting P^r as

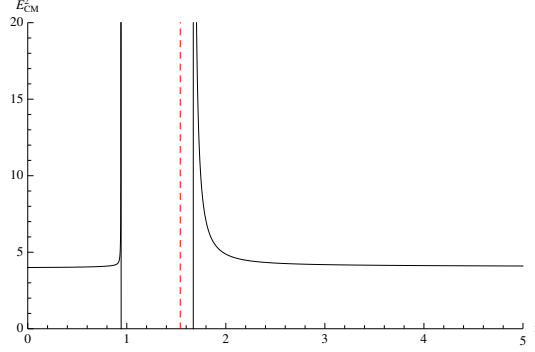


FIG. 9: The behavior of the E_{CM}^2 as a function of r , for $a_1 = -2$, $b_1 = 1$, $s_1 = 1$, $s_2 = 2.5$, $e_1 = e_2 = j_1 = j_2 = 1$, $m_1 = m_2 = 1$ and $\sigma = 0.1$. The red line corresponds to the event horizon radius $r_H \approx 1.54$. E_{CM}^2 diverges at the spin-related radius

$$\left(\frac{P^r}{m}\right)^2 = \frac{1 - \frac{as^2}{r^2}}{b^2 \left(1 - \frac{s^2}{2r} \left(a' + 2a\frac{b'}{b}\right)\right)^2} (e - V_+)(e - V_-), \quad (66)$$

where the effective potentials V_{\pm} are defined as

$$V_{\pm} = \left(1 - \frac{as^2}{r^2}\right)^{-1} \left((a'br^2 + 2ab'r^2 - 2abr) \frac{js}{2r^3} \pm \sqrt{a \left(1 + \frac{j^2}{r^2} - \frac{as^2}{r^2}\right) \left(1 - \frac{s^2}{2r} \left(a' + 2a\frac{b'}{b}\right)\right)^2} \right). \quad (67)$$

Notice that for the case $1 - as^2/r^2 > 0$, e must be bigger than V_+ or smaller than V_- for a real value of P^r . Therefore, from Eq. (51) and Eq. (52) we obtain the following set of momentum equations

$$\begin{aligned} \dot{P}^t + \left(\frac{a'}{2a} + \frac{b'}{b}\right) P^t \dot{r} + \left(\frac{a'}{2a} + \frac{b'}{b}\right) P^r \dot{t} &= \left(\frac{3a'b'}{2ab} + \frac{a''}{2a} + \frac{b''}{b}\right) S^{tr} \dot{r} + \left(a' + 2a\frac{b'}{b}\right) \frac{r}{2} S^{t\phi} \dot{\phi} \\ \dot{P}^r + \frac{1}{2} ab^2 \left(a' + 2a\frac{b'}{b}\right) P^t \dot{t} - \frac{a'}{2a} P^r \dot{r} - ra P^{\phi} \dot{\phi} &= a^2 b^2 \left(\frac{3a'b'}{2ab} + \frac{a''}{2a} + \frac{b''}{b}\right) S^{tr} \dot{t} + \frac{1}{2} ra' S^{r\phi} \dot{\phi} \\ \dot{P}^{\phi} + \frac{1}{r} P^r \dot{\phi} + \frac{1}{r} P^{\phi} \dot{r} &= -\frac{a'}{2ra} S^{r\phi} \dot{r} + \frac{ab^2}{2r} \left(a' + 2a\frac{b'}{b}\right) S^{t\phi} \dot{t} \end{aligned} \quad (68)$$

and the spin equations are given by

$$\begin{aligned} \dot{S}^{tr} + \frac{b'}{b} S^{tr} \dot{r} - ra S^{t\phi} \dot{\phi} &= P^t \dot{r} - P^r \dot{t} \\ \dot{S}^{r\phi} + \frac{1}{2} ab^2 \left(a' + 2a\frac{b'}{b}\right) S^{t\phi} \dot{t} + \left(-\frac{a'}{2a} + \frac{1}{r}\right) S^{r\phi} \dot{r} &= P^r \dot{\phi} - P^{\phi} \dot{r} \\ \dot{S}^{t\phi} + \frac{1}{r} S^{tr} \dot{\phi} + \left(\frac{a'}{2a} + \frac{b'}{b} + \frac{1}{r}\right) S^{t\phi} \dot{r} + \left(\frac{a'}{2a} + \frac{b'}{b}\right) S^{r\phi} \dot{t} &= P^t \dot{\phi} - P^{\phi} \dot{t}. \end{aligned} \quad (69)$$

These equations imply

$$\dot{r} = \frac{1 - \frac{a's^2}{2r} - \frac{as^2b'}{rb}}{1 - \frac{a's^2}{2r}} \frac{Pr}{P^t \dot{t}} \quad (70)$$

$$\dot{\phi} = -\frac{-2 + s^2 a'' + 3a' \frac{b'}{r} s^2 + 2a \frac{b''}{b} s^2}{2 \left(1 - \frac{a's^2}{2r}\right)} \frac{P\phi}{P^t \dot{t}}. \quad (71)$$

Using the above expressions we can evaluate the velocity square

$$\frac{u_\mu u^\mu}{(u^t)^2} = -a(r)b(r)^2 + \frac{1}{a(r)} \left(\frac{\dot{r}}{\dot{t}}\right)^2 + r^2 \left(\frac{\dot{\phi}}{\dot{t}}\right)^2. \quad (72)$$

In Fig. 10 we plot the behavior of $u_\mu u^\mu / (u^t)^2$ and Σ as a function of r and s for some small values of σ . The green surface corresponds to the behavior of $u_\mu u^\mu / (u^t)^2$ and the red surface corresponds to the behavior of Σ . The intersection between the green surface and the $z = 0$ horizontal plane is the limit where the trajectories change from timelike to spacelike character. The intersection between the red surface and the $z = 0$ horizontal plane corresponds to the values for which the CM energy diverges. We can observe that in order to reach a divergence in the energy of the center mass that the trajectory of the STOP has to pass from timelike to spacelike, which is similar to the collisions of spinning particles in the Schwarzschild background [30]. We recover the case for the Schwarzschild black hole when $\sigma = 0$, see the central panel of Fig. (10).

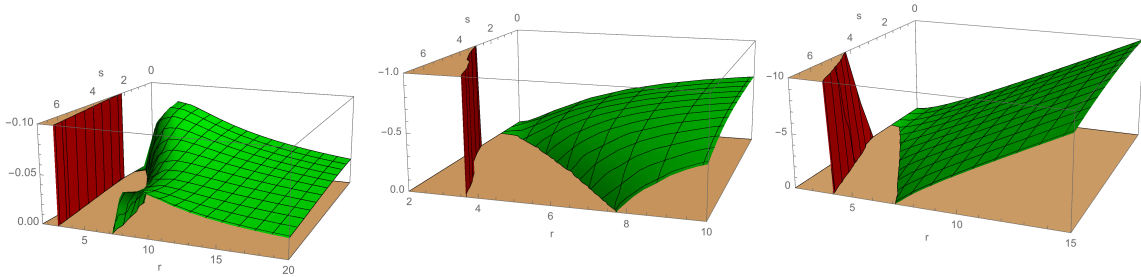


FIG. 10: The behavior of the velocity square $u_\mu u^\mu / (u^t)^2$ and Σ as a function of r and s , with $a_1 = -2M$, $M = 1$, $b_1 = 1$, $E = 1$, $j = -0.5$; left panel for $\sigma = 0.1$, central panel for $\sigma = 0$, and right panel for $\sigma = -0.1$.

V. CONCLUSIONS

In this paper we studied the motion of particles in the background of a DST black hole. We analyzed the motion of particles in the equatorial plane and we recovered the classical result of GR for $\sigma = 0$, and $r_S = 2M$ [42], recall $\sigma = 0$ corresponds to $\beta_n = 0$ due to its definition. A qualitative analysis of the effective potential for null geodesics shows that behavior for radial photons is similar to those in a Schwarzschild's spacetime [42]. The same occurs for the motion of photons with angular momentum, when $-1/2 < \sigma < 1/4$. Where, unstable circular orbits depend on the coupling parameter σ . However, for $\sigma < -1/2$, all orbits are bounded, which does not occur in the Schwarzschild's spacetime. The discrepancy between the theoretical value and the observational value of the deflection light was studied with respect to small deviations of Schwarzschild's spacetime. We have found via the geodesics formalism that the value of the coupling constant β_2 to match the theoretical result with the current observational constrains is $-8.97241 \times 10^{-6} \sqrt{3} \leq \beta_2 \leq 3.41708 \times 10^{-6} \sqrt{3}$.

Through the study for radial motion of massive particles we obtain new geodesics: for $\sigma < 0$ all orbits are bounded and for $0 < \sigma < 1/4$ appears an unstable equilibrium point (r_u), and two critical trajectories approaching to this point asymptotically with the same energy E_u . For particles with $E > E_u$, the trajectories are unbounded. For $E < E_u$, we showed that they allow a frontal scattering, that is characterized for incoming particles from infinity to a radial distance of closest approach, and come back to the infinity. With respect to the motion of particles with angular momentum and $\sigma < 0$, all trajectories are bounded due to potential at infinity, as for Schwarzschild AdS black hole [37] and the classical GR orbits are also allowed. Interestingly, for $0 < \sigma < 1/4$, the spacetime has two unstable circular orbits and one stable circular orbit, and as the potential vanishes at infinity, not all the orbits are bounded. Also, there are planetary orbits, which allowed us to study the perihelion precession for Mercury and the discrepancy between the theoretical and observational value, for small deviations of Schwarzschild's spacetime. In this regards, we found that it is possible attribute the discrepancy to a DST theory with a coupling constant $\beta_2 = 1.244 * 10^{-9} \sqrt{3}$. Due to the value of the coupling constant found for the perihelion precession is contained in the range obtained for the bending of light, these observables can be predicted by a unique DST theory according to observational data.

In consideration of the collision of spinning particles near the horizon and the possibility that the DST black hole acts as a particle accelerator, we showed that to reach a divergence in the center mass energy, the trajectory of the STOP has to pass from timelike to spacelike. Thus, for small deviations of General Relativity, the behavior is similar to the one observed for collisions of spinning particles in the Schwarzschild background [30].

Acknowledgments

We would like to thank Thomas Mädler for his comments and suggestions. This work is supported by Comisión Nacional de Ciencias y Tecnología of Chile through FONDECYT Grant N° 3170035 (A. Ö.), N° 1170279 (J. S.) and by the Dirección de Investigación y Desarrollo de la Universidad de La Serena (Y.V.). P. A. G. acknowledges the hospitality of the Universidad de La Serena where part of this work was undertaken. A. Ö. is grateful to Institute for Advanced

Study, Princeton for hospitality.

- [1] S. Deser, O. Sarioglu and B. Tekin, *Gen. Rel. Grav.* **40** (2008) 1.
- [2] H. Weyl, "Space-Time-Matter", New York: Dover, (1951).
- [3] T. Vetsov, arXiv:1806.05011 [gr-qc].
- [4] M. Olivares and J. R. Villanueva, *Eur. Phys. J. C* **73**, 2659 (2013) [arXiv:1311.4236 [gr-qc]].
- [5] P. A. Gonzalez, M. Olivares and Y. Vasquez, *Eur. Phys. J. C* **75**, no. 10, 464 (2015) [arXiv:1507.03610 [gr-qc]].
- [6] M. Mathisson, *Acta Phys. Polon.* 6, 163 (1937).
- [7] A. Papapetrou, *Proc. R. Soc. London, Ser. A*, 209, 248 (1951).
- [8] W. Tulczyjew, *Acta Phys. Polon.* 18, 393 (1959).
- [9] A. H. Taub, *J. Math. Phys.* 5, 112 (1964).
- [10] W. G. Dixon, *Riv. Nuovo Cimento Soc. Ital. Fis.* 34, 317 (1964).
- [11] E. Corinaldesi, and A. Papapetrou, *Proc. R. Soc. London, Ser. A*, 209, 259 (1951).
- [12] S. A. Hojman, PhD thesis, Princeton University (1975) (unpublished).
- [13] N. Zalaquett, S. A. Hojman and F. A. Asenjo, *Class. Quant. Grav.* **31**, 085011 (2014) doi:10.1088/0264-9381/31/8/085011 [arXiv:1308.4435 [gr-qc]].
- [14] R. Hojman, and S. A. Hojman, *Phys. Rev. D* 15, 2724 (1977).
- [15] M. Bañados, J. Silk and S. M. West, *Phys. Rev. Lett.* **103**, 111102 (2009) [arXiv:0909.0169 [hep-ph]].
- [16] T. Piran, J. Shaham and J. Katz. 1975. *Astrophys.J.*,196,L107
- [17] T. Piran and J. Shaham, *Phys. Rev. D* **16**, 1615 (1977). doi:10.1103/PhysRevD.16.1615
- [18] T. Piran and J. Shaham. 1977. *Astrophys.J.*,214,268
- [19] A. A. Grib and Y. V. Pavlov, *Int. J. Mod. Phys. D* **20**, 675 (2011) [arXiv:1008.3657 [gr-qc]].
- [20] O. B. Zaslavskii, *Phys. Rev. D* **82**, 083004 (2010) [arXiv:1007.3678 [gr-qc]].
- [21] O. B. Zaslavskii, *JETP Lett.* **92**, 571 (2010) [*Pisma Zh. Eksp. Teor. Fiz.* **92**, 635 (2010)] [arXiv:1007.4598 [gr-qc]].
- [22] S. Gao and C. Zhong, *Phys. Rev. D* **84**, 044006 (2011) [arXiv:1106.2852 [gr-qc]].
- [23] Y. Li, J. Yang, Y. L. Li, S. W. Wei and Y. X. Liu, *Class. Quant. Grav.* **28**, 225006 (2011) [arXiv:1012.0748 [hep-th]].
- [24] J. L. Said and K. Z. Adami, *Phys. Rev. D* **83**, 104047 (2011) [arXiv:1105.2658 [gr-qc]].
- [25] K. Lake, *Phys. Rev. Lett.* **104**, 211102 (2010) Erratum: [*Phys. Rev. Lett.* **104**, 259903 (2010)] [arXiv:1001.5463 [gr-qc]]. A. Abdujabbarov, B. Ahmedov and B. Ahmedov, *Phys. Rev. D* **84**, 044044 (2011) [arXiv:1107.5389 [astro-ph.SR]]. C. Zhong and S. Gao, *JETP Lett.* **94**, 589 (2011) [arXiv:1109.0772 [hep-th]]. Y. Zhu, S. Fengwu, Y. Xiao Liu, Y. Jiang, *Phys.Rev.D*84:043006,2011
- [26] A. Abdujabbarov, N. Dadhich, B. Ahmedov and H. Eshkuvatov, *Phys. Rev. D* **88**, 084036 (2013) [arXiv:1310.4494 [gr-qc]]. A. Galajinsky, *Phys. Rev. D* **88**, 027505 (2013) doi:10.1103/PhysRevD.88.027505 [arXiv:1301.1159 [gr-qc]]. S. R. Shaymatov, B. J. Ahmedov and A. A. Abdujabbarov, *Phys. Rev. D* **88**, no. 2, 024016 (2013). J. Sadeghi, B. Pourhassan and H. Farahani, *Commun. Theor. Phys.* **62**, no. 3, 358 (2014) [arXiv:1310.7142 [hep-th]]. S. Fernando, *Gen. Rel. Grav.* **46**, 1634 (2014) [arXiv:1311.1455 [gr-qc]]. J. Yang, Y. L. Li, Y. Li, S. W. Wei and Y. X. Liu, *Adv. High Energy Phys.* **2014**, 204016 (2014) [arXiv:1202.4159 [hep-th]]. S. G. Ghosh, P. Sheoran and M. Amir, *Phys. Rev. D* **90**, no. 10, 103006 (2014) [arXiv:1410.5588 [gr-qc]].
- [27] P. Pradhan, *Astropart. Phys.* **62**, 217 (2015) [arXiv:1407.0877 [gr-qc]]. P. Pradhan,

- arXiv:1402.2748 [gr-qc]. U. Debnath, arXiv:1508.02385 [gr-qc]. S. G. Ghosh and M. Amir, Eur. Phys. J. C **75**, no. 11, 553 (2015) [arXiv:1506.04382 [gr-qc]]. M. Amir and S. G. Ghosh, JHEP **1507**, 015 (2015) [arXiv:1503.08553 [gr-qc]]. B. Pourhassan and U. Debnath, arXiv:1506.03443 [gr-qc]. M. Guo and S. Gao, Phys. Rev. D **93**, no. 8, 084025 (2016) [arXiv:1602.08679 [gr-qc]]. Y. P. Zhang, B. M. Gu, S. W. Wei, J. Yang and Y. X. Liu, Phys. Rev. D **94**, no. 12, 124017 (2016) [arXiv:1608.08705 [gr-qc]]. O. B. Zaslavskii, EPL **114**, no. 3, 30003 (2016) [arXiv:1603.09353 [gr-qc]].
- [28] O. B. Zaslavskii, Int. J. Mod. Phys. D **26**, no. 10, 1750108 (2017) [arXiv:1602.08779 [gr-qc]]. N. Tsukamoto, K. Ogasawara and Y. Gong, Phys. Rev. D **96**, no. 2, 024042 (2017) [arXiv:1705.10477 [gr-qc]]. S. Fernando, Mod. Phys. Lett. A **32**, 1750074 (2017) [arXiv:1703.00373 [gr-qc]]. M. Halilsoy and A. Ovgun, Can. J. Phys. **95**, no. 11, 1037 (2017) [arXiv:1507.00633 [gr-qc]]. M. Halilsoy and A. Ovgun, Adv. High Energy Phys. **2017**, 4383617 (2017) [arXiv:1504.03840 [gr-qc]]. R. Becar, P. A. Gonzalez and Y. Vasquez, Eur. Phys. J. C **78**, no. 4, 335 (2018) [arXiv:1712.00868 [gr-qc]]. P. A. Gonzalez, M. Olivares, E. Papantonopoulos and Y. Vasquez, Phys. Rev. D **97**, no. 6, 064034 (2018) [arXiv:1802.01760 [gr-qc]].
- [29] F. Atamurotov, B. Ahmedov and S. Shaymatov, Astrophys. Space. Sci. **347**, 277 (2013)
- [30] C. Armaza, M. Bañados and B. Koch, Class. Quant. Grav. **33**, no. 10, 105014 (2016) [arXiv:1510.01223 [gr-qc]].
- [31] V. Perlick, Living Rev. Relativ. (2004) 7: 9.
- [32] V. Bozza, Gen. Rel. Grav. **42**, 2269 (2010).
- [33] Ivan Zh. Stefanov, Stoytcho S. Yazadjiev, and Galin G. Gyulchev, Phys. Rev. Lett. **104**:251103, (2010).
- [34] M. Bartelmann and P. Schneider, Phys. Rept. **340**, 291 (2001).
- [35] Straumann N.: General Relativity and Relativistic Astrophysics. Springer-Verlag, Berlin Heidelberg New York Tokio (1984).
- [36] J. R. Villanueva and M. Olivares, Eur. Phys. J. C **75**, no. 11, 562 (2015) [arXiv:1510.08340 [gr-qc]].
- [37] N. Cruz, M. Olivares and J. R. Villanueva, Class. Quant. Grav. **22**, 1167 (2005) [gr-qc/0408016].
- [38] S. Cornbleet, Am. J. Phys. **61**, 650 (1993);
- [39] R. Wald, *General Relativity*, University of Chicago Press, Chicago, 1984.
- [40] B. Shutz, *A First Course in General Relativity*, Cambridge University Press, 1990.
- [41] S. S. Shapiro, J. L. Davis, D. E. Lebach and J. S. Gregory, Phys. Rev. Lett. **92**, 121101 (2004).
- [42] Chandrasekhar S.: The Mathematical Theory of Black Holes. Oxford University Press, New York (1983).